Harnessing atomistic simulations to predict the rate at which dislocations overcome obstacles

S. Saroukhani [a,*], L.D. Nguyen [a], K.W.K. Leung [a], C.V. Singh [b], D.H. Warner [a]

[a] School of Civil and Environmental Engineering, Cornell University, Ithaca, NY 14853, USA
[b] Department of Materials Science and Engineering, University of Toronto, Toronto, Ontario, Canada M5S 3E4

ARTICLE INFO

ABSTRACT

Predicting the rate at which dislocations overcome obstacles is key to understanding the microscopic features that govern the plastic flow of modern alloys. In this spirit, the current manuscript examines the rate at which an edge dislocation overcomes an obstacle in aluminum. Predictions were made using different popular variants of Harmonic Transition State Theory (HTST) and compared to those of direct Molecular Dynamics (MD) simulations. The HTST predictions were found to be grossly inaccurate due to the large entropy barrier associated with the dislocation–obstacle interaction. Considering the importance of finite temperature effects, the utility of the Finite Temperature String (FTS) method was then explored. While this approach was found capable of identifying a prominent reaction tube, it was not capable of computing the free energy profile along the tube. Lastly, the utility of the Transition Interface Sampling (TIS) approach was explored, which does not need a free energy profile and is known to be less reliant on the choice of reaction coordinate. The TIS approach was found capable of accurately predicting the rate, relative to direct MD simulations. This finding was utilized to examine the temperature and load dependence of the dislocation–obstacle interaction in a simple periodic cell configuration. An attractive rate prediction approach combining TST and simple continuum models is identified, and the strain rate sensitivity of individual dislocation obstacle interactions is predicted.

© 2016 Elsevier Ltd. All rights reserved.

1. Introduction

The outcome of dislocation–obstacle interactions can be highly sensitive to the nanoscale details of the interaction (Singh and Warner, 2010; Singh et al., 2011). This motivates the use of atomistic modeling techniques to study these interactions. A key challenge for the atomistic modeling approach is that dislocation motion across obstacles is a thermally activated event, and hence rare in the time-scale accessible to direct atomistic modeling. This motivates the development and application of indirect atomistic modeling techniques, aimed at computing the rate at which dislocations overcome obstacles.

One of the most common indirect atomistic modeling approaches to compute the rates of thermally activated events is Harmonic Transition State Theory (HTST). HTST assumes that the reaction rate is governed by a single energy barrier that separates the initial (unreacted) and final (reacted) states of the system. Further, HTST assumes that the potential energy surface is quadratic at the initial and saddle configurations. This equates to approximating the activation entropy by the

---

vibrational entropy and neglecting anharmonic effects such as thermal expansion (Vineyard, 1957), an approximation often believed to be accurate for solids (Voter, 1997b; Delph et al., 2013). This approach produces a rate expression similar to that of the Arrhenius equation involving a pre-exponential factor and an activation potential energy. The latter can be accurately calculated using minimum energy path techniques such as the Nudged Elastic Band (NEB) method (Jonsson et al., 1998) and the 0 K String method (Weinan et al., 2002). Calculating the pre-exponential factor requires solving two eigenvalue problems for the normal frequencies of the system near the initial and saddle configurations.

The eigenvalue problems are formidable for large systems and hence are often avoided in practice (Hirel et al., Aug 2008; Gordon et al., 2008; Rodney, 2007; Zhu et al., 2004; Hara and Li, 2010). A common approach for avoiding the large eigenvalue problem is to approximate the pre-exponential factor by the normal frequency along the reaction coordinate at the initial state (Hara and Li, 2010). This is equivalent to assuming that the entropy barrier is zero. Other approximations for the pre-exponential factor such as the imaginary frequency of the saddle configuration (Rodney, 2007), continuum estimates (Zhu et al., 2004), and the Debye frequency have also been used in the literature. Henceforth, we will refer to these approaches as Simplified HTST (SHTST).

Due to the approximations mentioned above, the HTST and SHTST approaches are not universally able to accurately predict reaction rates in solids. A recent example is the prediction of dislocation nucleation rates, which has been shown to have large entropic barriers due to anharmonic effects (Nguyen et al., 2011; Nguyen and Warner, 2012; Warner and Curtin, 2009; Hara and Li, 2010; Ryu et al., 2011a; Kim and Tadmor, 2014). In these cases, other approaches such as Parallel Replica Dynamics (PRD) (Voter, 1998; Warner and Curtin, 2009), Hyperdynamics (Voter, 1997b, 1997a; Hara and Li, 2010; Baker and Warner, 2012) and Transition State Theory (TST) combined with different free energy calculation techniques such as the Finite Temperature String (FTS) method (Ren and Vanden-Eijnden, 2005, 2005b) and Umbrella Sampling (Frenkel and Smit, 2001) have been successfully used to predict rates from atomistic simulations. However, each of these methods is known to have certain restrictions, which limit their accuracy and applications in a consistent manner. For instance, PRD provides a speedup that at most scales with the number of replicas used and hence can only handle problems with high rates and small activation volumes. The Hyperdynamics approach, on the other hand, needs an artificial potential that is application specific and non-trivial to design. Finally, TST strongly relies on the choice of reaction coordinate and a dividing surface, i.e. a transition bottleneck, which can be challenging to define.

To overcome the challenges involved in the above methods, path sampling techniques have drawn significant attention in the biophysics and chemistry communities (Escobedo et al., 2009; Juraszek et al., 2012; Best, 2012; Bolhuis, 2003; Borrero and Escobedo, 2006; Schwartz and Schramm, 2009; Basner and Schwartz, 2005). A major advantage is that these methods do not need a carefully defined reaction coordinate and prior knowledge on the transition path and mechanism. They are based on the fact that a transition is fully characterized by the transition path ensemble (TPE). In other words, the TPE contains the information needed to predict all transition features such as reaction coordinate(s), rate(s), free energy profile (s) and mechanism(s) (Peters and Trout, 2006; van Erp et al., 2003; Bolhuis and Dellago, 2011; Dellago et al., 1998a; Allen et al., 2009; Dellago et al., 1999, 1998b). Comprehensive reviews of such methods can be found in Escobedo et al. (2009), Moroni (2005), Bolhuis and Dellago (2011), Bertini and Reiher (2007), Bolhuis and Dellago (2009), and Dellago and Bolhuis (2009). Nevertheless, these techniques have not so far been utilized for understanding phenomena underlying plasticity and fracture in metallic systems. In this manuscript, the TPE approach known as Transition Interface Sampling (van Erp et al., 2003) will be utilized to predict the rate at which an edge dislocation overcomes an obstacle.

This paper examines the application of HTST, TST, and TIS to predict the rate at which an edge dislocation overcomes an obstacle. The manuscript begins with a brief description of the theoretical background of each method. Atomistic simulation details are given in Section 3. In Section 4.1, HTST, TST, and TIS predictions are compared to that of direct molecular dynamics (MD) simulations for a benchmark problem. The entropy barrier of the problem and the validity of the harmonic approximation are examined in Section 4.2. In Section 4.3, the rate calculation is applied to predict the strain rate sensitivity (SRS) factor for an Al–Cu alloy, which can be compared to experimental measurements. The final section draws some conclusions from the analyses and points out potential future directions.

2. Methods

2.1. Transition state theory

Transition State Theory (TST) provides an exact expression for the rate at which an ergodic system crosses a dividing surface, S_D, partitioning the configuration space into two sets a and b:

$$k_{ab}[S_D] = \sqrt{\frac{K_B T}{2m\pi}} \frac{Z_{S_D}}{Z_a} \tag{1}$$

with k_B being the Boltzmann constant, T being the temperature, m being the effective mass, $Z_{S_D} = \int_{S_D} e^{-\frac{V(\mathbf{x})}{k_B T}} d\sigma(\mathbf{x})$ and $Z_a = \int_a e^{-\frac{V(\mathbf{x})}{k_B T}} d\mathbf{x}$ are the constrained partition functions associated with S_D and a respectively. The term $\sqrt{\frac{K_B T}{2m\pi}}$ is the flux

through the dividing surface and $\frac{Z_{S_D}}{Z_a}$ represents the probability of the system being on S_D relative to a (Glasstone et al., 1941; Eyring, 1935; Wigner, 1938; Horiuti, 1938; Moroni, 2005; Bolhuis and Dellago, 2011). Often, a surface, S_0, which does not intersect S_D and contains an initial configuration in a, is defined to express Eq. (1) in terms of a free energy barrier (Moroni, 2005; Vineyard, 1957):

$$k_{ab}[S_D] = \tilde{\nu} e^{-\frac{\Delta F}{k_B T}} \tag{2}$$

where

$$\tilde{\nu} = \sqrt{\frac{K_B T}{2m\pi}} Z_a^{-1} \int_{S_0} e^{-\frac{V(\mathbf{x})}{k_B T}} \, d\sigma(\mathbf{x}) \tag{3}$$

and the free energy barrier is

$$\Delta F = F_{S_D} - F_{S_0} = - k_B T \ln\left(\frac{\int_{S_D} e^{-\frac{V(\mathbf{x})}{k_B T}} \, d\sigma(\mathbf{x})}{\int_{S_0} e^{-\frac{V(\mathbf{x})}{k_B T}} \, d\sigma(\mathbf{x})} \right) \tag{4}$$

which can also be written as

$$\Delta F(\sigma, T) = \Delta U(\sigma, T) - T\Delta S(\sigma, T) \tag{5}$$

with $\Delta U(\sigma, T)$ being the activation internal energy and $\Delta S(\sigma, T)$ the activation entropy. It should be noted that $\tilde{\nu}$, ΔF, ΔU and ΔS are not intrinsic properties of the system with respect to S_D as they depend on S_0. In practice, however, these quantities are often not appreciably dependent on the choice of S_0 so long as it is physically reasonable, e.g. passing through the minimum energy state in a and normal to an appropriate reaction coordinate.

One challenge in computing the rate from Eq. (2) is that one is often interested in the transition rate between two metastable regions $A \subset a$ and $B \subset b$ that do not necessarily partition the phase space and hence a transition cannot be exactly characterized by crossing a hypersurface. In such cases, the flux through the dividing surface is an upper bound to the flux from one metastable state to another because trajectories might recross S_D multiple times before committing to B or may not commit to B at all. Therefore, the TST rate formula, Eq. (2), can overestimate the actual rate of interest, i.e.

$$k_{AB} \leq k_{ab}[S_D] \tag{6}$$

A standard approach for dealing with the above challenge is the Bennett–Chandler (BC) TST method (Bennett, 1977; Chandler, 1978; Moroni, 2005) whereby the flux through S_D is modified such that only trajectories that reach the final state are counted and multiple recrossings are counted only once. The latter is done by weighting forward and backward crossings with different signs such that they cancel out. In practice, this amounts to scaling $k_{ab}[S_D]$ by the probability, κ, that each crossing towards B leads to a transition, meaning

$$k_{AB} \approx \kappa k_{ab}[S_D] \tag{7}$$

where $\kappa = \lim_{N \to \infty} \frac{2N_B}{N}$, a.k.a. the transmission coefficient, is computed by starting a large number, N, of trajectories from an equilibrium distribution on S_D and counting the number, N_B, that commit to B in a time $t^* \ll 1/(k_{AB} + k_{BA})$. For the BC-TST approach to be effective, the dividing surface, S_D, must be chosen such that κ is close to one. In other words, S_D must be a bottleneck for the transition such that trajectories crossing it have a high probability of committing to B. Otherwise, an infeasible number of trajectories are needed to compute κ accurately. It is worth noting that there are more efficient approaches for defining κ based on the *effective positive flux* formalism (Van Erp and Bolhuis, 2005), which avoids counting positive and negative crossings by only counting the first *positive* crossing for *effective* trajectories (Bolhuis and Dellago, 2011).

A less demanding approach is the Variational TST (VTST) that assumes $\kappa = 1$ and chooses S_D as the surface, $S_D^{\min}$, that minimizes the transition frequency, $\nu = k_{ab}[S_D]Z_a$ (Vanden-Eijnden and Tal, 2005; Truhlar and Garrett, 1980). Considering the TST rate formula, Eq. (2), $S_D^{\min}$ is the surface that minimizes $\int_{S_D} e^{-\frac{V(\mathbf{x})}{k_B T}} \, d\sigma(\mathbf{x})$ and hence has the highest free energy. In other words, VTST assumes that the bottleneck characterized by S_D that needs to be overcome for the transition to happen is the activation free energy. In order to find this surface, one needs to compute a free energy profile along a properly chosen reaction coordinate, λ, whereby $S_D^{\min}$ can be taken as the level set, $\lambda = \lambda^*$, with the highest free energy. The Finite Temperature String (FTS) method described in the next subsection can be used for this purpose.

The demanding task of computing a free energy profile for the above methods motivates the Harmonic TST (HTST) approach, which avoids this task by assuming that the potential energy surface is quadratic at the initial and saddle configurations. This assumption amounts to temperature independent material properties and is widely used for problems involving solids. The method further assumes that the dividing surface corresponds to a potential energy ridge, S_D^V, between A and B to express the transition rate as

$$k_{AB} \approx \left(\frac{\prod_{i=1}^{3N} \nu_i^{\text{initial}}}{\prod_{i=1}^{3N-1} \nu_i^{\text{saddle}}} \right) e^{-\frac{\Delta V}{k_B T}} = \nu_0 e^{-\frac{\Delta V}{k_B T}}$$

(8)

where ν_i^{initial} and ν_i^{saddle} are respectively the normal frequencies of the system in the initial configuration and the minimum potential energy configuration within S_D^V, i.e. the saddle configuration. The product over the saddle point frequencies excludes the imaginary frequency in the direction of the reaction coordinate, i.e. normal to S_D^V, and hence all frequencies are real. N is the number of atoms in the system and ΔV is the difference in the potential energy between the saddle and initial configurations.

Solving the two eigenvalue problems required for Eq. (8) becomes prohibitively expensive for large systems. That is why Eq. (8) is sometimes further simplified by assuming that the prefactor is equal to the normal frequency, ν_*^{initial}, in the direction of the reaction coordinate in the initial state:

$$k_{AB} \approx \nu_*^{\text{initial}} e^{-\frac{\Delta V}{k_B T}}$$

(9)

We will refer to this approach as the Simplified HTST (SHTST). Other choices for the pre-factor such a continuum estimate, the imaginary frequency of the saddle point, or the Debye frequency have also been used in the literature (Hara and Li, 2010; Rodney, 2007; Zhu et al., 2004; Gordon et al., 2008).

2.2. Finite temperature string method

FTS is an algorithm for finding a reaction coordinate and computing the free energy profile along the coordinate. It has been extensively used with TST to predict reaction rates (Nguyen and Warner, 2012; Nguyen et al., 2011; Ren et al., 2005a; Qian et al., 2005). The method utilizes the idea of reaction tubes, a relatively high probability region in configuration space that links A and B. Assuming that reaction tubes are thin and isolated, the method offers an algorithm for finding iso-committer surfaces, i.e. surfaces where the probability that a trajectory reaches B before A is uniform, and the expected configuration on each of them. A reaction coordinate is then defined as a curve (string) connecting the expected configurations. We refer the interested reader to references Ren and Vanden-Eijnden (2005), Ren and Vanden-Eijnden (2005b), Ren et al. (2005a), Vanden-Eijnden and Venturoli (2009), and Weinan et al. (2007) for further details on the theoretical background of the method.

The algorithm starts with an initial string connecting the initial and final states through a set of equally spaced intermediate configurations (images) and a set of Voronoi cells centered at the images. Constrained sampling at constant temperature is performed within each cell and the time averaged position associated with each cell is computed. Then, the time averaged positions are used to update the string and Voronoi cells, while satisfying a smoothing condition and enforcing equal distance between images. Iterating over this process leads to a converged string and its associated Voronoi cells. The Voronoi cells approximate the iso-committer surfaces and the images approximate the expected configuration within them. The quality of the approximation depends on the discretization error and the sampling error. Further details of the algorithm can be found in Vanden-Eijnden and Venturoli (2009) and Ren et al. (2005a).

FTS also offers an algorithm for calculating the free energy profile. The algorithm uses the global balance equation,

$$\sum_{\substack{\alpha'=0 \\ \alpha' \neq \alpha}}^{N} \pi_{\alpha} k_{\alpha'\alpha} = \sum_{\substack{\alpha'=0 \\ \alpha' \neq \alpha}}^{N} \pi_{\alpha} k_{\alpha\alpha'}$$

(10)

together with

$$\sum_{\alpha=0}^{N} \pi_{\alpha} = 1$$

(11)

to find the equilibrium probabilities, π_{α}, of the cells $\alpha = 0, ..., N$. The transition matrix, $k_{\alpha\alpha'}$, can be computed from the formula

$$k_{\alpha\alpha'} = \frac{N_{\alpha\alpha'}^n}{n \Delta t}$$

(12)

by initiating a trajectory inside cell α and counting the number of times, $N_{\alpha\alpha'}^n$, the trajectory enters cell α' over n timesteps of Δt. When the trajectory leaves the cell where it was initiated, which is α in this case, it is brought back to the last configuration it had before leaving the cell. The estimate in Eq. (12) converges as the length of the trajectory goes to infinity, i.e. $n \to \infty$. Further details can be found in Vanden-Eijnden and Venturoli (2009).

2.3. Transition interface sampling

Like TST based approaches, TIS aims to calculate a flux, but it does not require a transition state to be identified a priori nor does it require a carefully chosen reaction coordinate and the computation of the free energy profile along the

coordinate (van Erp et al., 2003). These advantages stem from the fact that the method directly calculates the rate using actual trajectories of the system, i.e. samples of the Transition Path Ensemble (TPE). TIS measures the flux through a set of hypersurfaces partitioning phase space rather than a single dividing surface, which can be hard to define. The TIS method is based on the *effective positive flux* formalism (Bolhuis and Dellago, 2011; Van Erp and Bolhuis, 2005) which makes it less sensitive to recrossings.

The first step in TIS is to partition phase space using a set of $n + 1$ non-intersecting interfaces, defined as level sets of an order parameter, $\lambda(\mathbf{x})$, i.e. $\lambda_i = \{\mathbf{x}|\lambda(\mathbf{x}) = \lambda_i\}$, $i = 0, \ldots, n$. The order parameter, $\lambda(\mathbf{x})$, does not have to be associated with a properly chosen reaction coordinate; it is sufficient that $\lambda(\mathbf{x})$ characterizes the basins of attraction of A and B (Moroni, 2005; van Erp et al., 2003; Van Erp and Bolhuis, 2005). As schematically shown in Fig. 2, each interface, λ_i, is closer to A than the next interface, λ_{i+1}, such that $\lambda_0 = \lambda_A$ defines the boundary of the basin of attraction of A and $\lambda_n = \lambda_B$ defines that of B.

TIS makes use of the *effective positive flux* formalism to express the transition rate as

$$k_{AB} = \frac{\langle \phi_{\lambda_0, \lambda_n} \rangle}{\langle h_{\mathcal{A}} \rangle} \tag{13}$$

where $h_{\mathcal{A}}$ is the indicator function and $\phi_{\lambda_0, \lambda_n}$ is the *effective positive flux* from state A through interface λ_n (van Erp et al., 2003). $\mathcal{A}$ is the set of all phase points where the corresponding trajectories come from A without having visited B. A transition happens when the system leaves $\mathcal{A}$, i.e. when the system enters B for the first time. The denominator, $\langle h_{\mathcal{A}} \rangle$, is the fraction of time the system spends in $\mathcal{A}$. Therefore, Eq. (13) is the exact definition of rate, which is the number of *effective* transitions from A to B divided by the total time the system spends in $\mathcal{A}$, in the limit of time going to infinity. It is also worth noting that the equation is equivalent to the TST rate formula when $S_D = \lambda_A = \lambda_B$, i.e. when the transition is characterized by crossing a single dividing surface.

Calculating the rate from Eq. (13) is not feasible as it requires simulations that are long enough to capture a rare transition. To overcome this challenge, TIS relates the flux through an interface, λ_i, to that of the previous interface, λ_{i-1}, using the recursive formula

$$\langle \phi_{\lambda_0, \lambda_i} \rangle = \langle \phi_{\lambda_0, \lambda_{i-1}} \rangle P(\lambda_i | \lambda_{i-1}) \tag{14}$$

where $P(\lambda_i | \lambda_{i-1})$ is the probability that a trajectory, coming from A, crosses λ_i provided that it has already crossed λ_{i-1} (van Erp et al., 2003; Moroni et al., 2004; Borrero et al., 2011). For instance in Fig. 2, $p(\lambda_4 | \lambda_3)$ is the fraction of blue trajectories to the red and blue trajectories. In simpler words, this equation relates the flux through two neighbor interfaces by using the fact that only a fraction of trajectories that cross λ_{i-1} make it to λ_i before going back to A. That fraction is the probability $P(\lambda_i | \lambda_{i-1})$. Using the recursive formula in Eq. (14), we can express $\langle \phi_{\lambda_0, \lambda_n} \rangle$ as

$$\langle \phi_{\lambda_0, \lambda_n} \rangle = \langle \phi_{\lambda_0, \lambda_1} \rangle \prod_{i=1}^{n-1} P(\lambda_{i+1} | \lambda_i) \tag{15}$$

and hence rewrite Eq. (13) as

$$k_{AB} = \frac{\langle \phi_{\lambda_0, \lambda_1} \rangle}{\langle h_{\mathcal{A}} \rangle} \prod_{i=1}^{n-1} P(\lambda_{i+1} | \lambda_i) \tag{16}$$

where the term $\frac{\langle \phi_{\lambda_0, \lambda_1} \rangle}{\langle h_{\mathcal{A}} \rangle}$ is the rate of transition from λ_0 to λ_1, which can be computed using direct MD simulations.

The trajectories needed for calculating the probabilities $P(\lambda_{i+1} | \lambda_i)$ cannot be generated using direct simulations for interfaces that are far from A. A method commonly used for this purpose in the TIS literature is the so-called 'shooting move', which is a Metropolis Markov Chain Monte Carlo (MCMC) algorithm. The theoretical and algorithmic details of the method can be found in van Erp et al. (2003) and Bolhuis et al. (2002). The algorithm ensures generating samples from the Boltzmann distribution by satisfying the detailed balance equation and using the Boltzmann distribution for deriving the acceptance rule. Like other MCMC algorithms, the shooting move suffers from correlated samples, which slow down convergence and impede exploring multiple reaction channels.

Path Swapping TIS (PSTIS) is one approach to attempt to overcome the correlation problem. It is based on the idea that trajectories that have crossed an interface, λ_i, might also cross the neighboring interfaces, λ_{i-1} and λ_{i+1}. In other words, trajectories in an ensemble, $P(\lambda_{i+1} | \lambda_i)$, might also be in the neighboring ensembles, $P(\lambda_i | \lambda_{i-1})$ and $P(\lambda_{i+2} | \lambda_{i+1})$. This means an ensemble can exchange samples, i.e. trajectories, with its neighbors. In that case, a new sample is added to each of the ensembles without performing the most expensive step of the shooting move, i.e. the integration. This also alleviates the correlation problem and increases the chance of exploring multiple reaction tubes. Further details on the algorithm can be found in van Erp (2007).

3. Simulation details

The atomistic simulations were conducted using a modified version of the LAMMPS package and an angular dependent embedded atom method (EAM) empirical potential developed by Apostol and Mishin (2011). The simulation cell consisted
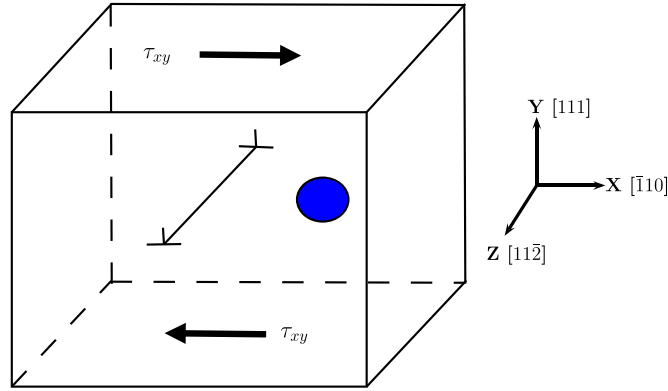
Fig. 1. Simulation cell with an edge dislocation and a precipitate.

of an edge dislocation in an FCC Al lattice and a mono-layer Cu obstacle representing a GP-zone. The simulation box, Fig. 1, contained approximately 13,000 atoms in total, with 13 Cu atoms in the obstacle. The box was bounded by $(1\bar{1}0)$, (111), and $(\bar{1}\bar{1}2)$ faces in the X, Y, and Z directions, respectively. The GP-zone lied on the (100) plane. An edge dislocation was created with a line direction parallel to the Z-axis and $b = 1/2[\bar{1}10]$. Periodic boundary conditions were applied in the X and Z directions. The system was loaded by applying the shear forces

$$f_{top} = \frac{\tau_{xy} A_{xz}}{N_{top}}, \quad f_{bottom} = -\frac{\tau_{xy} A_{xz}}{N_{bottom}}$$

(17)

on the atoms near the top and bottom Y surfaces, while the displacements of the atoms in those layers are determined by the dynamics of the system.

Direct MD simulations were performed with NVT dynamics where a Langevin thermostat with a damping parameter of 1 ps was used. The NVT ensemble was chosen because of implementation convenience. As proved in Ryu et al. (2011b), the choice of the ensemble does not affect the activation free energy and hence the rate, but the entropy barriers are different. Our analysis showed that the choice does not affect the conclusions drawn about temperature effects in Section 4.2. Further, convergence studies with respect to the loading rate were conducted to ensure the fidelity of the rate predictions.

As mentioned in Section 2, HTST and TST rate expressions involve the potential and free energy barriers respectively. The potential energy barrier ΔV is computed using the 0 K string method (Weinan et al., 2002), which is equivalent to the Nudged Elastic Band (NEB) approach (Jonsson et al., 1998). The FTS method is used to obtain a reaction coordinate and compute the free energy profile, as discussed in Section 2.2. Both versions of the string method require an initial string connecting the initial and final configurations through a set of intermediate ones. This string has been generated by interpolation using the Euclidean norm.

The set of interfaces for TIS was simply defined as the boundaries between Voronoi cells of the convergent string given by the FTS method. The string was also used as the initial trajectory needed to start the shooting move. The simulations to compute $P_A(\lambda_{i+1}|\lambda_i)$ for each λ_i were performed in parallel. For each λ_i, five to ten 1 ns simulations, started at different seeds, were performed. The transition flux through the first interface, $\frac{\langle \phi_{\lambda_0,\lambda_1} \rangle}{\langle h_A \rangle}$, was calculated using 50 independent direct MD simulations started at different seeds.

Table 1
The predictions of the methods described in Section 2 for the average time, $\bar{t}$, for an edge dislocation to overcome an obstacle at $\tau_{xy} = 200$ MPa and $T = 300$ K.

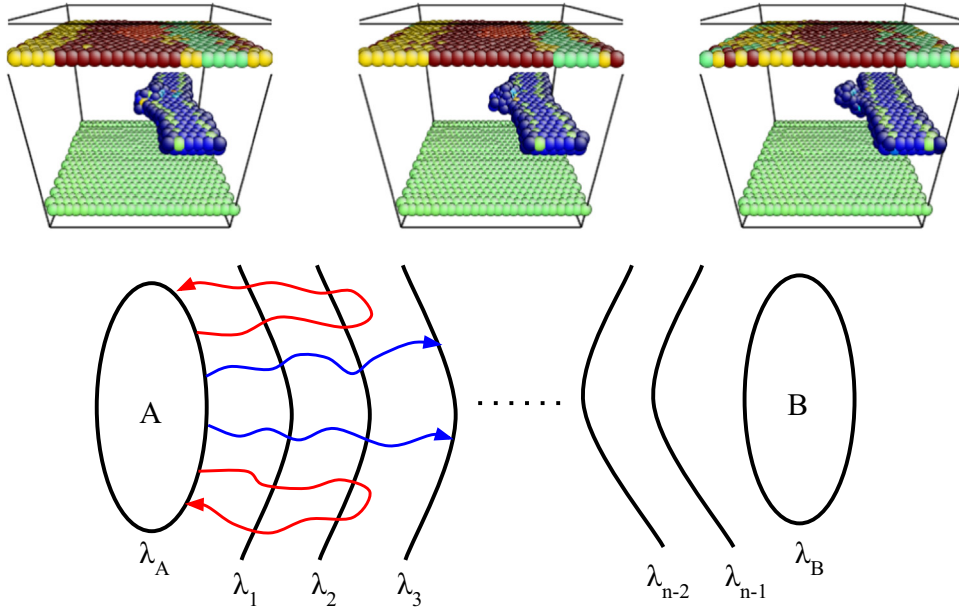| Method	$\bar{t}$ (ns)
Direct MD	8.99
PSTIS	3.8
TIS	2.27
HTST	1.48×10^{14}
SHTST	1.26×10^{11}
FTS	N/A

Fig. 2. *Bottom*: A schematic picture of the interfaces and trajectories involved in TIS calculations. The interfaces are the boundaries of the cells defined by the FTS method. The blue and red trajectories have been described in Section 2. *Top*: Snapshots of the system as the dislocation overcomes the obstacle at $\tau_{xy} = 200$ MPa and T=300 K. The left image is the initial configuration where the first partial dislocation has overcome the obstacle and the second partial has not. The right image is the final configuration where the second partial has overcome the obstacle. The middle image is the center of one of the intermediate cells. The images have been plotted by AtomEye (Li, 2003). Only atoms not in a perfect FCC stacking, i.e. having a large centro-symmetry parameter, are shown. (For interpretation of the references to color in this figure caption, the reader is referred to the web version of this paper.)

4. Results and discussion

4.1. Comparison of the methods

The performance of the methods described in Section 2 was examined by comparing their predictions of the average time for a dislocation to overcome an obstacle, $\bar{t} = k_{AB}^{-1}$, to a benchmark obtained by direct MD simulations at $\tau_{xy} = 200$ MPa and $T=300$ K (Table 1). The choice of the load was based on the limited time-scale accessible to MD simulations and the athermal critical shear stress, $\hat{\tau} = 300$ MPa. In this case, the rate controlling event was observed to be the second partial dislocation overcoming the obstacle through Orowan looping (Singh and Warner, 2013). Therefore, the results may be generalized to other strong obstacles lying on other planes. Fig. 2 shows the initial, final and an intermediate configuration of the system, plotted using AtomEye (Li, 2003). The benchmark was obtained by running 50 statistically independent direct MD simulations and averaging the transition time, i.e. the time for the second partial to overcome the obstacle.

As shown in Table 1, HTST overestimated $\bar{t}$ by about 13 orders of magnitude relative to the direct MD prediction. The activation energy obtained by the 0 K string method was $\Delta V = 0.91$ eV. The pre-exponential factor ν_0 obtained by solving for $\nu_i^{initial}$ and ν_i^{saddle} in Eq. (8) was 1.3×10^{10} s^{-1}. A SHTST prediction based on the Debye frequency of Aluminum, 1.54×10^{13} s^{-1}, is also shown in the table, which overestimates $\bar{t}$ by 11 orders of magnitude. As discussed in the next subsection, the inaccuracy of the HTST predictions is due to the large entropic barrier due to thermal softening, which is neglected by the harmonic approximation.

Our efforts to compute a free energy profile using FTS were frustrated. Although the method results in a converged reaction coordinate (string) in the first stage of the algorithm, the constrained sampling of the second stage fails to obtain a converged transition matrix. We believe that this problem stems from the failure of key FTS assumptions. First, reaction tubes are assumed to be separated by energy barriers significantly larger than the thermal energy so that trajectories do not leave the tube where they were initiated. Second, reaction tubes are assumed to be thin so that iso-committor surfaces can be approximated by hyperplanes. A consequence of these assumptions is that the sampling trajectories must spend most of their time near their respective cell centers. This means that the time averaged positions of the sampling trajectories will form a smooth curve along the cells. A feature that was not observed in the simulations performed here.

It should be noted that failure in obtaining a converged transition matrix does not contradict a convergent string in the first stage for two reasons. First, there is a smoothing term in the first stage that ensures the time averaged positions of neighbor cells are smoothly connected; whereas, there is no such constraint when calculating the transition matrix. Further, in the first stage, trajectories making a transition to a new tube do not remain there long enough to change their respective cell centers. This is because trajectories are brought back to their cell centers as soon as they leave the cells. When calculating the transition matrix, on the other hand, trajectories are brought back to the last configuration they had before leaving
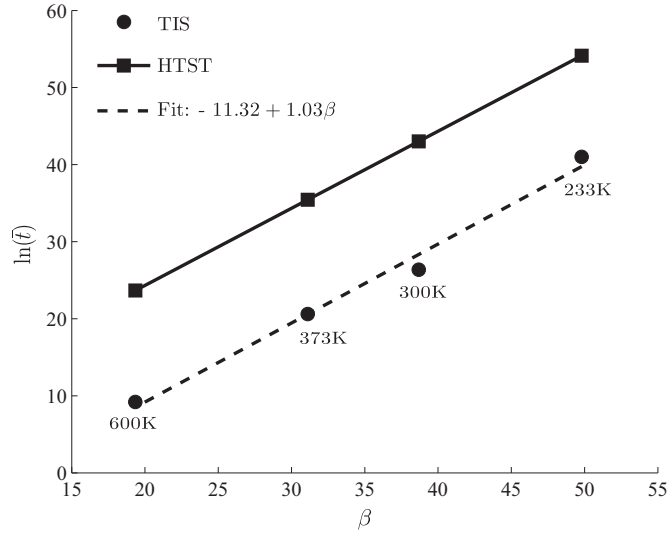
Fig. 3. HTST (solid line) and TIS (dashed line) Arrhenius plots. HTST (squares) and TIS (circles) predictions have been computed at four temperatures: 233 K, 300 K, 373 K and 600 K. The average time, $\bar{t}$, is in picoseconds.

their cells, which could be far from the cell centers.

TIS performs better than the other methods and provides a fairly accurate prediction of the average time, $\bar{t}$. This is because TIS does not rely on prior knowledge about the transition such as the reaction coordinate, free energy profile, transition state and the nature of the entropy barrier. Instead, it directly computes the flux characterizing the rate using real trajectories of the system, i.e. samples of the Transition Path Ensemble (TPE). The success of the TIS approach and the failure of the TST-FTS approach shows the importance of this level of generality.

We believe that a considerable amount of the error in the TIS prediction is due to the correlated nature of the trajectories used to estimate $P(\lambda_{i+1}|\lambda_i)$. As mentioned in Section 2, TIS makes use of an MCMC algorithm for generating trajectories of the system and hence the convergence is slowed down by the correlated nature of successive samples. Moreover, the correlation issue leads to most TIS trajectories lying in one reaction tube and not exploring others. As mentioned in Section 2, the Path Swapping version of TIS, which we call PSTIS, has been proposed to alleviate the correlation problem and facilitate exploring multiple reaction tubes. As shown in Table 1, the method proves to be effective at improving the time average prediction in this problem.

4.2. Temperature effect

To gain insight into the energetics associated with a dislocation overcoming an obstacle and the performance of the various rate prediction methods, the temperature dependence of the rate was examined. To this end, TIS rate predictions were carried out at four temperatures and placed on an Arrhenius plot with HTST predictions, i.e. $\ln(\bar{t})$ versus $\beta = 1/k_B T$ (Fig. 3). The simulations were performed at a constant shear stress of $\tau_{xy} = 120$ MPa, with the potential energy barrier being $\Delta V = 1.0$ eV. The shear stress is about 3/4 of the yield strength in shear of underaged Al-4wt.%Cu, which is the closest Al–Cu alloy to the cell considered here.

Interestingly, the TIS predictions follow a linear trend on the Arrhenius plot, with the same slope as the HTST prediction, i.e. 1.0 eV. This implies that $\Delta U(\sigma, T)$, $\tilde{\nu}(\sigma, T)$ and $\Delta S(\sigma, T)$ are likely to be temperature independent over the range examined, considering that

$$\ln(\bar{t}) = -\ln[\tilde{\nu}(\sigma, T)] - \frac{\Delta S(\sigma, T)}{k_B} + \beta \Delta U(\sigma, T) \tag{18}$$

from Eq. (5), $\bar{t} = 1/k^{\text{TST}}$, and Eq. (2). Accordingly, the y-intercept then represents the quantity $-\left(\ln[\tilde{\nu}(\sigma, T)] + \frac{\Delta S(\sigma, T)}{k_B}\right)$, which can also be interpreted as the natural log of the prefactor in the Arrhenius equation for a process with a temperature independent energy barrier. The linear fit of the TIS data on the Arrhenius plot has a y-intercept of -11.3. This value is considerably below HTST intercept of 4.3 ($-\ln(\nu_0)$), and represents the main source of error in the HTST rate predictions.

Considering that $\tilde{\nu}(\sigma, T)$ can be easily computed from direct MD simulation, $\Delta S(\sigma, T)$ can be obtained. At $T = 300$ K, we found $\tilde{\nu} \approx 1.5 \times 10^{11}\,\text{s}^{-1}$. Therefore, the entropy barrier is $\Delta S = 13.2 k_B$, a value significantly beyond the 1–2 k_B range associated with the typical vibrational entropy of solids (Ryu, 2011; Hara and Li, 2010).

The large entropy barrier likely results from the nature of the dislocation–obstacle interaction and the temperature dependence of the shear modulus and stacking fault energies (Yamakov et al., 2014). Specifically, the activated state involves

an increased dislocation length relative to the initial state. This makes the free energy of the activated state more temperature dependent than the free energy of the initial state, which is described by a large entropy difference between the two states.

This idea is consistent with traditional continuum thermoelastic models, e.g. DiMelfi et al. (1976), Surek et al. (1973), and Schoeck (1965). These models express the activation free energy as a function of the shear modulus, $\mu(T)$, as $\Delta F(\sigma, T) = \Delta V(\sigma) \frac{\mu(T)}{\mu(0)}$ (Argon, 2008; Ryu, 2011). Based on this expression for ΔF and the assumption that μ linearly decreases with temperature and vanishes at the melting point T_m (Argon, 2008; Yamakov et al., 2014; Muraishi et al., 2002), the activation entropy is modeled as

$$\Delta S(\sigma) = \frac{\Delta V(\sigma)}{T_m} \tag{19}$$

This expression is equivalent to the 'thermodynamic compensation law' or the Meyer-Neldel rule, which is an empirical relation that has proved valid for many thermally activated processes.

Based on the melting point of Al-4wt.%Cu, $T_m = 933$ K (Meyrick and Powell, 1973), the entropy barrier estimated by Eq. (19) is $12.4 k_B$. This value is very similar to that obtained with Eq. (18) using the TIS approach. Furthermore, the model describes a temperature independent activation entropy, consistent with the TIS predictions.

These results not only illuminate the powerful utility of the Meyer–Neldel rule for predicting the rate at which dislocations overcome obstacles, but they show that the large entropy barrier associated with the phenomenon can be explained by the anharmonic effect of thermal softening.

4.3. Load effect

The applied load is an important factor that controls the rate at which dislocations overcome obstacles. Macroscopically, this effect manifests itself in the dependence of the plastic strain rate, $\dot{\epsilon}_p$, on the applied stress, τ, and is characterized by a strain rate sensitivity (SRS) factor, $m = \frac{\partial \ln \tau}{\partial \ln \dot{\epsilon}_p}$, an experimentally measured quantity. $\dot{\epsilon}_p$ is proportional to the average velocity of dislocations, v. In alloys that are governed by dislocation–obstacle interactions, such as underaged Al-4wt.%Cu, a first order approximation of v under ordinary loading conditions is $v \approx d/\bar{t}$, with d being the average obstacle spacing in the glide direction of the mobile dislocations. Thus, m can be estimated directly from the TIS results that provide the stress dependence of $\bar{t}$.

Alternatively, m is commonly predicted from TST (Xu and Picu, 2007). Often, $\tilde{\nu}$ is assumed to be stress independent and the form of ΔF is chosen based upon specific features of the system (Kocks, 1975). This allows m to be written as $m = -k_B T \frac{\partial \ln \tau}{\partial \Delta F}$. For a periodic array of weak obstacles, a widely used form for the stress dependence of ΔF is Friedel's model,

$$\Delta F = \Delta F_0 \left(1 - \frac{\tau}{\hat{\tau}} \right)^{\frac{3}{2}} \tag{20}$$

where the activation energy at zero stress, ΔF_0, is a fitting parameter and $\hat{\tau}$ is the athermal critical shear stress.

TIS rate predictions across six different stress levels at $T = 300$ K were examined within the context of the above assumptions (Fig. 4). Specifically, the $\bar{t}$ predictions were plugged into the TST rate formula, Eq. (2), and ΔF was solved for at the different stress levels. The ΔF versus τ data is also shown in Fig. 4. Using $\Delta F_0 = 1.7$ eV, the data is described well by Friedel's model across a wide range of stresses.
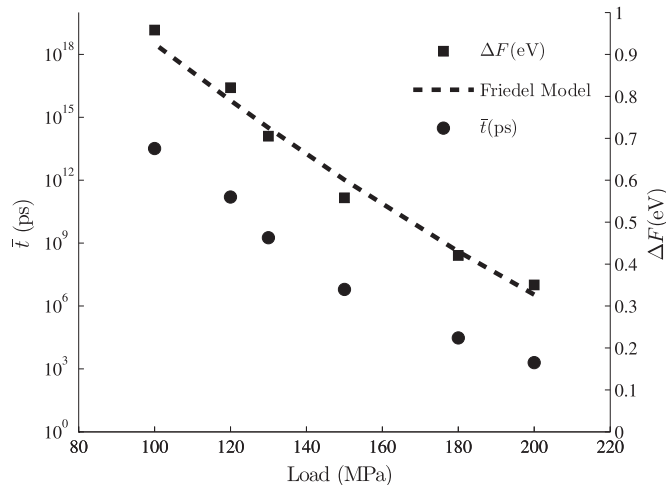

Fig. 4. Activation energy and average time vs load at 300 K.

The SRS factor, *m*, associated with the TIS predictions is between 0.03 and 0.05 depending upon the applied load, noting that similar results are obtained whether computing m directly from the TIS data or using the TST approach with Friedel's model. Our predictions of m are almost an order of magnitude higher than those observed in room temperature experiments on traditional aluminum alloys hardened by dislocation precipitate interactions, $m \approx 0.005$ (Muraishi et al., 2002; Byrne et al., 1961). This disconnect suggests that the experimentally measured strain rate sensitivity of such materials is not governed by the strain rate sensitivity of individual dislocation–obstacle interactions. This finding supports the hypothesis proposed by Picu et al. (2009), Xu and Picu (2007), and Weiss et al. (2007), that the strain rate sensitivity of many engineering alloys may instead by governed by the correlated motion of dislocations through a random field of obstacles. With that said, the reader is reminded that artificial boundary effects associated with the small periodic simulation cell utilized here might also be important (Szajewski and Curtin, 2015).

5. Summary and conclusions

This manuscript documents our attempt to use atomistic simulation to predict the rate at which dislocations overcome obstacles. We began by considering the most common rate prediction approach for solids, HTST. For a small example problem that could be solved with direct MD, we found HTST incapable of predicting the rate. Hypothesizing that the harmonic approximation was the source of the error, the TST approach was then attempted. We were unable to predict the rate with the TST approach due to our inability to calculate a free energy profile along a reaction coordinate identified with the FTS method. We believe that the FTS approach was impeded by the failure of its key assumptions for this application. This motivated us to explore the TIS approach, which utilizes actual reactive trajectories to predict the rate. The TIS approach was found capable of accurately predicting the rate that dislocations overcome obstacles, relative to direct MD simulation. To better explore the energy landscape and improve the rate predictions, a path swapping algorithm was ultimately utilized within the TIS framework.

Having established the accuracy of TIS predictions for the application, the TIS approach was used to examine the temperature dependence of the dislocation–obstacle interaction and the validity of the harmonic approximation. To that end, TIS was used to generate an Arrhenius plot, which was compared to HTST predictions. The TIS plot was linear with the same slope as the HTST prediction, but with a different intercept. This suggests that the phenomenon of a dislocation overcoming an obstacle consists of a large entropy barrier that is temperature independent. The temperature dependence of the associated free energy barrier was found to be accurately described by standard continuum models that include a thermal softening effect.

The TIS approach was also used to examine the stress dependence of the rate. The results were found to be well described by TST and Friedel's model for the stress dependence of the free energy barrier. The strain rate sensitivity for a dislocation to overcome a row of periodic obstacles in aluminum is predicted to be between $m=0.03$ and $m=0.05$ at room temperature, a finding that can aid the quest to better understand the processes that control the strength of real-world engineering alloys.

In closing, we have shown that the TIS approach is capable of accurately predicting the rate at which dislocations overcome obstacles and that simple continuum models are capable of describing the temperature and stress dependence of the rate. The latter finding establishes an attractive approximate approach for predicting the rate, i.e. using TST in careful combination with the simple continuum models examined here. For other problems where this is not the case or known, path sampling techniques such as TIS are attractive alternatives to TST-based approaches as they offer a much higher degree of generality for the same amount of implementation efforts.

Acknowledgments

References

Allen, R.J., Valeriani, C., ten Wolde, P.R., 2009. Forward flux sampling for rare event simulations. J. Phys.: Condens. Matter 21 (46), 463102.
Apostol, F., Mishin, Y., 2011. Interatomic potential for the Al–Cu system. Phys. Rev. B 83 (5), 054116.
Argon, A.S., 2008. Strengthening Mechanisms in Crystal Plasticity, vol. 4. Oxford University Press, Oxford.
Baker, K., Warner, D., 2012. Extended timescale atomistic modeling of crack tip behavior in aluminum. Model. Simul. Mater. Sci. Eng. 20 (6), 065005.
Basner, J.E., Schwartz, S.D., 2005. How enzyme dynamics helps catalyze a reaction in atomic detail: a transition path sampling study. J. Am. Chem. Soc. 127 (40), 13822–13831.
Bennett, C., 1977. Algorithms for chemical computations. In: ACS symposium Series. vol. 46. p. 63.
Bertini, L., Reiher, M., 2007. Atomistic Approaches in Modern Biology: From Quantum Chemistry to Molecular Simulations, vol. 268. Springer, Berlin.
Best, R.B., 2012. Atomistic molecular simulations of protein folding. Curr. Opin. Struct. Biol. 22 (1), 52–61.
Bolhuis, P.G., 2003. Transition-path sampling of β-hairpin folding. Pro. Natl. Acad. Sci. 100 (21), 12129–12134.
Bolhuis, P.G., Chandler, D., Dellago, C., Geissler, P.L., 2002. Transition path sampling: throwing ropes over rough mountain passes, in the dark. Annu. Rev. Phys. Chem. 53 (1), 291–318. pMID: 11972010, URL ⟨http://www.annualreviews.org/doi/abs/10.1146/annurev.physchem.53.082301.113146⟩.
Bolhuis, P.G., Dellago, C., 2011. 3 trajectory-based rare event simulations. Rev. Comput. Chem. 27, 111.

Bolhuis, P.G., Dellago, C., Dünweg, B., Gompper, G., Ihle, T., Kroll, D., Ladd, A., Winkler, R., 2009. Advanced Computer Simulation Approaches for Soft Matter Sciences III. Self 221.

Borrero, E.E., Escobedo, F.A., 2006. Folding kinetics of a lattice protein via a forward flux sampling approach. J. Chem. Phys. 125 (16), 164904.

Borrero, E.E., Weinwurm, M., Dellago, C., 2011. Optimizing transition interface sampling simulations. J. Chem. Phys. 134 (24), 244118.

Byrne, J., Fine, M., Kelly, A., 1961. Precipitate hardening in an aluminium–copper alloy. Philos. Mag. 6 (69), 1119–1145.

Chandler, D., 1978. Statistical mechanics of isomerization dynamics in liquids and the transition state approximation. J. Chem. Phys. 68 (6), 2959–2970.

Dellago, C., Bolhuis, P.G., 2009. Transition path sampling and other advanced simulation techniques for rare events. In: Advanced Computer Simulation Approaches for Soft Matter Sciences III. Springer, Berlin, pp. 167–233.

Dellago, C., Bolhuis, P.G., Chandler, D., 1998a. Efficient transition path sampling: application to Lennard–Jones cluster rearrangements. J. Chem. Phys. 108 (22), 9236–9245.

Dellago, C., Bolhuis, P.G., Chandler, D., 1999. On the calculation of reaction rate constants in the transition path ensemble. J. Chem. Phys. 110 (14), 6617–6625.

Dellago, C., Bolhuis, P.G., Csajka, F.S., Chandler, D., 1998b. Transition path sampling and the calculation of rate constants. J. Chem. Phys. 108 (5), 1964–1977.

Delph, T., Cao, P., Park, H., Zimmerman, J., 2013. A harmonic transition state theory model for defect initiation in crystals. Model. Simul. Mater. Sci. Eng. 21 (2), 025010.

DiMelfi, R., Nix, W., Barnett, D., Holbrook, J., Pound, G., 1976. An analysis of the entropy of thermally activated dislocation motion based on the theory of thermoelasticity. Phys. Status Solidi (B) 75 (2), 573–582.

Escobedo, F.A., Borrero, E.E., Araque, J.C., 2009. Transition path sampling and forward flux sampling. Applications to biological systems. J. Phys.: Condens. Matter 21 (33), 333101.

Eyring, H., 1935. The activated complex in chemical reactions. J. Chem. Phys. 3 (2), 107–115.

Frenkel, D., Smit, B., 2001. Understanding Molecular Simulation: from Algorithms to Applications, vol. 1. Academic Press, Orlando, FL.

Glasstone, S., Laidler, K.J., Eyring, H., 1941. The Theory of Rate Processes: The Kinetics of Chemical Reactions, Viscosity, Diffusion and Electrochemical Phenomena. McGraw-Hill Book Company, Incorporated, New York.

Gordon, P.A., Neeraj, T., Luton, M.J., 2008. Atomistic simulation of dislocation nucleation barriers from cracktips in α-fe. Model. Simul. Mater. Sci. Eng. 16 (4), 045006.

Hara, S., Li, J., 2010. Adaptive strain-boost hyperdynamics simulations of stress-driven atomic processes. Phys. Rev. B 82 (18), 184114.

Hirel, P., Godet, J., Brochard, S., Pizzagalli, L., Beauchamp, P., Aug 2008. Determination of activation parameters for dislocation formation from a surface in fcc metals by atomistic simulations. Phys. Rev. B 78, 064109. ⟨http://link.aps.org/doi/10.1103/PhysRevB.78.064109⟩.

Horiuti, J., 1938. On the statistical mechanical treatment of the absolute rate of chemical reaction. Bull. Chem. Soc. Jpn. 13 (1), 210–216.

Jonsson, H., Mills, G., Jacobsen, K.W., 1998. Nudged Elastic Band Method for Finding Minimum Energy Paths of Transitions.

Juraszek, J., Vreede, J., Bolhuis, P.G., 2012. Transition path sampling of protein conformational changes. Chem. Phys. 396, 30–44.

Kim, W.K., Tadmor, E.B., 2014. Entropically stabilized dislocations. Phys. Rev. Lett. 112 (10), 105501.

Kocks, W., 1975. Thermodynamics and kinetics of slip. Progr. Mater. Sci. 19, 291.

Li, J., 2003. Atomeye: an efficient atomistic configuration viewer. Model. Simul. Mater. Sci. Eng. 11 (2), 173.

Meyrick, G., Powell, G.W., 1973. Phase transformations in metals and alloys. Annu. Rev. Mater. Sci. 3 (1), 327–362.

Moroni, D., 2005. Efficient sampling of rare event pathways (Ph.D. thesis), Universiteit van Amsterdam.

Moroni, D., van Erp, T.S., Bolhuis, P.G., 2004. Investigating rare events by transition interface sampling. Physica A: Stat. Mech. Appl. 340 (1), 395–401.

Muraishi, S., Niwa, N., Maekawa, A., Kumai, S., Sato, A., 2002. Strengthening of Al–Cu single crystals by stress-oriented Guinier–Preston zones. Philos. Mag. A 82 (14), 2755–2771.

Nguyen, L., Baker, K., Warner, D., 2011. Atomistic predictions of dislocation nucleation with transition state theory. Phys. Rev. B 84 (2), 024118.

Nguyen, L., Warner, D., 2012. Improbability of void growth in aluminum via dislocation nucleation under typical laboratory conditions. Phys. Rev. Lett. 108 (3), 035501.

Peters, B., Trout, B.L., 2006. Obtaining reaction coordinates by likelihood maximization. J. Chem. Phys. 125 (5), 054108.

Picu, R., Li, R., Xu, Z., 2009. Strain rate sensitivity of thermally activated dislocation motion across fields of obstacles of different kind. Mater. Sci. Eng.: A 502 (1–2), 164–171. URL ⟨http://www.sciencedirect.com/science/article/pii/S0921509308012434⟩.

Qian, T., Ren, W., Sheng, P., 2005. Current dissipation in thin superconducting wires: a numerical evaluation using the string method. Phys. Rev. B 72 (1), 014512.

Ren, W., Vanden-Eijnden, E., 2005. Finite temperature string method for the study of rare events. J. Phys. Chem. B 109 (14), 6688–6693.

Ren, W., Vanden-Eijnden, E., Maragakis, P., Weinan, E., et al., 2005a. Transition pathways in complex systems: application of the finite-temperature string method to the alanine dipeptide. J. Chem. Phys. 123 (13), 134109.

Ren, W., Vanden-Eijnden, E., et al., 2005b. Transition pathways in complex systems: reaction coordinates, isocommittor surfaces, and transition tubes. Chem. Phys. Lett. 413 (1), 242–247.

Rodney, D., 2007. Activation enthalpy for kink-pair nucleation on dislocations: comparison between static and dynamic atomic-scale simulations. Phys. Rev. B 76 (October), 144108. URL ⟨http://link.aps.org/doi/10.1103/PhysRevB.76.144108⟩.

Ryu, S., 2011. The Validity of Classical Nucleation Theory and its Application to Dislocation Nucleation. Stanford University.

Ryu, S., Kang, K., Cai, W., 2011a. Entropic effect on the rate of dislocation nucleation. Proc. Natl. Acad. Sci. 108 (13), 5174–5178.

Ryu, S., Kang, K., Cai, W., 2011b. Predicting the dislocation nucleation rate as a function of temperature and stress. J. Mater. Res. 26 (18), 2335–2354.

Schoeck, G., 1965. The activation energy of dislocation movement. Physica Status Solidi (B) 8 (2), 499–507.

Schwartz, S.D., Schramm, V.L., 2009. Enzymatic transition states and dynamic motion in barrier crossing. Nat. Chem. Biol. 5 (8), 551–558.

Singh, C., Mateos, A., Warner, D., 2011. Atomistic simulations of dislocation–precipitate interactions emphasize importance of cross-slip. Scr. Mater. 64 (5), 398–401.

Singh, C., Warner, D., 2010. Mechanisms of Guinier–Preston zone hardening in the athermal limit. Acta Mater. 58 (17), 5797–5805.

Singh, C.V., Warner, D.H., 2013. An atomistic-based hierarchical multiscale examination of age hardening in an Al–Cu alloy. Metall. Mater. Trans. A 44 (6), 2625–2644.

Surek, T., Luton, M., Jonas, J., 1973. Dislocation glide controlled by linear elastic obstacles: a thermodynamic analysis. Philos. Mag. 27 (2), 425–440.

Szajewski, B., Curtin, W., 2015. Analysis of spurious image forces in atomistic simulations of dislocations. Model. Simul. Mater. Sci. Eng. 23 (2), 025008.

Truhlar, D.G., Garrett, B.C., 1980. Variational transition-state theory. Acc. Chem. Res. 13 (12), 440–448.

van Erp, T.S., 2007. Reaction rate calculation by parallel path swapping. Phys. Rev. Lett. 98 (May), 268301.

Van Erp, T.S., Bolhuis, P.G., 2005. Elaborating transition interface sampling methods. J. Comput. Phys. 205 (1), 157–181.

van Erp, T.S., Moroni, D., Bolhuis, P.G., 2003. A novel path sampling method for the calculation of rate constants. J. Phys. Chem. 118 (May), 7762–7774.

Vanden-Eijnden, E., Tal, F.A., 2005. Transition state theory: variational formulation, dynamical corrections, and error estimates. J. Chem. Phys. 123 (18), 184103.

Vanden-Eijnden, E., Venturoli, M., 2009. Revisiting the finite temperature string method for the calculation of reaction tubes and free energies. J. Chem. Phys. 130 (19), 194103.

Vineyard, G.H., 1957. Frequency factors and isotope effects in solid state rate processes. J. Phys. Chem. Solids 3 (1), 121–127.

Voter, A., 1997a. Hyperdynamics: accelerated molecular dynamics of infrequent events. Phys. Rev. Lett. 78 (May), 3908–3911. URL ⟨http://link.aps.org/doi/10.1103/PhysRevLett.78.3908⟩.

Voter, A., 1998. Parallel replica method for dynamics of infrequent events. Phys. Rev. B 57 (June), R13985–R13988. URL ⟨http://link.aps.org/doi/10.1103/PhysRevB.57.R13985⟩.

Voter, A.F., 1997b. A method for accelerating the molecular dynamics simulation of infrequent events. J. Chem. Phys. 106 (11), 4665–4677.

Warner, D., Curtin, W., 2009. Origins and implications of temperature-dependent activation energy barriers for dislocation nucleation in face-centered cubic metals. Acta Mater. 57 (14), 4267–4277.

Weinan, E., Ren, W., Vanden-Eijnden, E., 2002. String method for the study of rare events. Phys. Rev. B 66 (5), 052301.

Weinan, E., Ren, W., Vanden-Eijnden, E., 2007. Simplified and improved string method for computing the minimum energy paths in barrier-crossing events. J. Chem. Phys. 126 (16), 164103.

Weiss, J., Richeton, T., Louchet, F., Chmelik, F., Dobron, P., Entemeyer, D., Lebyodkin, M., Lebedkina, T., Fressengeas, C., McDonald, R.J., 2007. Evidence for universal intermittent crystal plasticity from acoustic emission and high-resolution extensometry experiments. Phys. Rev. B 76 (22), 224110.

Wigner, E., 1938. The transition state method. Trans. Faraday Soc 34, 29–41.

Xu, Z., Picu, R., 2007. Thermally activated motion of dislocations in fields of obstacles: the effect of obstacle distribution. Phys. Rev. B 76 (September), 094112. URL ⟨http://link.aps.org/doi/10.1103/PhysRevB.76.094112⟩.

Yamakov, V., Warner, D., Zamora, R., Saether, E., Curtin, W., Glaessgen, E., 2014. Investigation of crack tip dislocation emission in aluminum using multiscale molecular dynamics simulation and continuum modeling. J. Mech. Phys. Solids 65, 35–53.

Zhu, T., Li, J., Yip, S., 2004. Atomistic study of dislocation loop emission from a crack tip. Phys. Rev. Lett. 93 (July), 025503. URL ⟨http://link.aps.org/doi/10.1103/PhysRevLett.93.025503⟩.